◆ Human Brain Mapping 6:14–32(1998) ◆

Dissociation of Mnemonic and Perceptual Processes During Spatial and Nonspatial Working Memory Using fMRI

Aysenil Belger,[1,3]* Aina Puce,[2,4] John H. Krystal,[3] John C. Gore,[5] Patricia Goldman-Rakic,[6] and Gregory McCarthy[2,4]

[1]*Cognitive Neuroscience Laboratory, VA Medical Center, West Haven, Connecticut 06516*
[2]*Neuropsychology Laboratory, VA Medical Center, West Haven, Connecticut 06516*
[3]*Department of Psychiatry, Yale University School of Medicine, New Haven, Connecticut 06510*
[4]*Department of Neurosurgery, Yale University School of Medicine, New Haven, Connecticut 06510*
[5]*Department of Diagnostic Radiology, Yale University School of Medicine, New Haven, Connecticut 06510*
[6]*Department of Neurobiology, Yale University School of Medicine, New Haven, Connecticut 06510*

Abstract: Neuroimaging studies in humans have consistently found robust activation of frontal, parietal, and temporal regions during working memory tasks. Whether these activations represent functional networks segregated by perceptual domain is still at issue. Two functional magnetic resonance imaging experiments were conducted, both of which used multiple-cycle, alternating task designs. Experiment 1 compared spatial and object working memory tasks to identify cortical regions differentially activated by these perceptual domains. Experiment 2 compared working memory and perceptual control tasks within each of the spatial and object domains to determine whether the regions identified in experiment 1 were driven primarily by the perceptual or mnemonic demands of the tasks, and to identify common brain regions activated by working memory in both perceptual domains. Domain-specific activation occurred in the inferior parietal cortex for spatial tasks, and in the inferior occipitotemporal cortex for object tasks, particularly in the left hemisphere. However, neither area was strongly influenced by task demands, being nearly equally activated by the working memory and perceptual control tasks. In contrast, activation of the dorsolateral prefrontal cortex and the intraparietal sulcus (IPS) was strongly task-related. Spatial working memory primarily activated the right middle frontal gyrus (MFG) and the IPS. Object working memory activated the MFG bilaterally, the left inferior frontal gyrus, and the IPS, particularly in the left hemisphere. Finally, activation of midline posterior regions, including the cingulate gyrus, occurred at the offset of the working memory tasks, particularly the shape task. These results support a prominent role of the prefrontal and parietal cortices in working memory, and indicate that spatial and object working memory tasks recruit differential hemispheric networks. The results also affirm the distinction between spatial and object perceptual processing in dorsal and ventral visual pathways. *Hum. Brain Mapping 6:14–32, 1998.*

Key words: prefrontal cortex; posterior parietal cortex; inferior temporal cortex; spatial working memory; nonspatial working memory; functional MRI

INTRODUCTION

Efficient information processing requires the integration of sensory inputs that reach central processing systems at different times and locations. This integra-

Contract grant sponsor: Department of Veterans Affairs; Contract grant sponsor: NIMH; Contract grant numbers: MH-44866, MH-05286.

*Correspondence to: Aysenil Belger, Ph.D., Psychiatry Service 116A1, VA Medical Center, 950 Campbell Avenue, West Haven, CT 06516. E-mail: Belger@npl.med.yale.edu

Received for publication 23 July 1997; Accepted 17 September 1997

tive process relies upon temporary storage systems, such as those defined by Baddeley [1986] as ''working memory.'' Neurobiological studies in nonhuman primates have provided evidence that working memory functions assessed by spatial delayed-response tasks recruit a complex network of regions, including the posterior parietal and dorsolateral prefrontal regions (dPFC) [Goldman-Rakic, 1987; Fuster, 1989, 1995]. Neurons in monkey dPFC increase their firing rate during the delay period of spatial delayed match-to-sample tasks beyond the perceptual processing period [Fuster, 1973; Quintana et al., 1988; Funahashi et al., 1989]. Recent studies have demonstrated that spatial and nonspatial delayed response tasks activate different populations of neurons within the prefrontal cortex, with a domain-differential distribution in dorsal and ventral prefrontal regions, respectively [Wilson et al., 1993; cf. Rao et al., 1997]. Studies in monkeys have also shown dissociation of these two processing domains in the posterior brain, where the parietal cortex is critical for the processing of spatial information and the inferior occipitotemporal cortex (IOTC) is critical for visual feature analysis [Ungerleider and Mishkin, 1982]. Thus, reciprocal cortico-cortical connections between the parietal and prefrontal cortex [Selemon and Goldman-Rakic, 1988; Cavada and Goldman-Rakic, 1989] and between the inferior temporal lobes and PFC [Kawamura and Naito, 1984; Barbas, 1988; Barbas and Mesulam, 1981; Webster et al., 1994] may form the respective anatomical bases for spatial and object working memory networks.

The present study has two aims. The first is to extend our previous analysis of differential dPFC activation during spatial and object working memory tasks [McCarthy et al., 1996] to parietal and temporal regions. In addition, we sought to determine the degree to which activation observed in these regions was dependent upon perceptual vs. mnemonic processing. Numerous imaging studies have observed activations in these posterior regions during working memory tasks [e.g., Jonides et al., 1993; Smith et al., 1996; Swartz et al., 1994, 1995]. However, to date only Goldberg et al. [1996] have attempted to dissociate activations due to the perceptual and mnemonic demands of working memory tasks. Since extrastriate and superior parietal activation during a spatial delayed-match task exceeded activation during their perceptual control task, Goldberg et al. [1996] concluded that these regions interact with the prefrontal cortex to maintain spatial information ''on-line.''

The second aim of the present experiments is to reexamine the loci of activation during spatial and object processing within the prefrontal cortex. The emergence of the critical role of the prefrontal cortex in delayed-matching tasks in nonhuman primates has prompted numerous neuroimaging studies in humans which demonstrated differential activation of PFC during spatial tasks, and during nonspatial tasks accessing verbal, phonological, and object working memory [Zatorre et al., 1992; Jonides et al., 1993; Petrides et al., 1993a,b; Cohen et al., 1994; McCarthy, 1995; McCarthy et al., 1994, 1996; Swartz et al., 1994, 1995; Smith et al., 1996; D'Esposito et al., 1995]. Nevertheless, discrepancies remain with respect to the detailed anatomical localization of these activations. Some studies have reported primarily ventrolateral frontal activation (BA 47) [Jonides et al., 1993; Smith et al., 1995], others have reported middle frontal gyrus (MFG) activation [McCarthy et al., 1994, 1996; Petrides et al., 1993a; Cohen et al., 1994], and yet others have reported a lack of activation in prefrontal regions during working memory tasks [Courtney et al., 1996].

Owen et al. [1996] suggested that these discrepancies could be partially explained by the differences in task characteristics which differentially accessed planning and mnemonic capacities of the frontal lobes. According to Owen et al., [1996] ventrolateral frontal regions (BA 47) subserve the interaction between short-term and long-term memory systems and executive processing, such as those involved in the delayed-matching tasks utilized by Jonides et al. [1993] among others. In contrast, dorsolateral prefrontal regions (BA 46) would subserve the interaction between executive processes and memory systems when active manipulation of information within working memory is required, such as during continuous performance tasks as used by McCarthy et al. [1994, 1996]. We address this proposal by comparing the prefrontal loci of activation from our prior continuous performance tasks to the delayed-matching task design used here.

The present studies use an alternating task paradigm to investigate networks for spatial and object working memory in which subjects continuously switched between spatial (location) and object (shape) delayed-matching tasks and perceptual control tasks. This design emphasizes brain regions *differentially* activated by the two conditions while deemphasizing commonly activated regions. In experiment 1, spatial and object working memory tasks were alternated, thus emphasizing differences related to the perceptual processing domain. Regions activated by the working memory demands common to both perceptual domains would be deemphasized. Experiment 2 compared working memory and nonmemory perceptual control tasks within each processing domain, thus emphasizing differences related to memory demands.

By comparing the outcomes of both experiments, we attempted to identify regions engaged by working memory and differentiated by processing domain (spatial vs. object). Following Goldberg et al. [1996], we were particularly interested in determining whether inferior temporal regions activated during feature analysis and parietal regions activated by spatial analysis were affected by the imposition of the cognitive demands of a working memory task.

MATERIALS AND METHODS

Subjects

A total of 18 right-handed subjects (11 females), ranging in age from 20–35 years, participated in experiment 1, with 10 subjects participating in a frontal lobe imaging session (experiment 1A), and 14 subjects participating in a posterior brain imaging session (experiment 1B). Six subjects participated in both sessions. Twelve subjects (6 females), ranging in age between 18–35 years, participated in experiment 2. Ten of these subjects were right-handed. All subjects had normal or corrected-to-normal visual acuity. The experimental protocol was approved of by the Yale University School of Medicine Human Investigation Committee, and all subjects provided informed consent.

Experiment 1 tasks

In experiment 1, subjects performed a continuous series of working memory tasks which alternated between spatial (location) and nonspatial (shape) processing domains. In the location working memory task, a sequence of three white squares appeared at three randomly chosen locations on the screen (Fig. 1). Each square appeared for 0.5 sec and the interstimulus interval (ISI) between successive squares was also 0.5 sec. The offset of the third square was followed by a blank retention delay interval of 3.5 sec, which ended with the presentation of a red target square. The target square, also displayed for 0.5 sec, matched the location of one of the three preceding white squares on half of the trials.

The shape working memory task used identical timing as the location task (Fig. 1), with the following stimulus modifications. The three successive stimuli consisted of white abstract shapes (polygons with 3–7 vertices) which appeared at the center of the screen. The red target shape appeared at center screen and matched one of the previous three shapes on half of the trials. For both location and shape working memory tasks, subjects were instructed to maintain central fixation and indicate whether the target matched, or did not match, one of the three test stimuli, by depressing one of two buttons of a fiber-optic response box.

All stimuli were randomly generated for each trial and thus were not repeated during the experiment. A small fixation cross was visible at the center of the display during the entire duration of the location task, and during all ISIs of the shape task. The subjects were instructed to fixate during both tasks.

The total duration of each task trial was 8.73 sec, consisting of the presentation of the three test stimuli, the delay interval, the target, and a response interval following target offset. A *run* consisted of an alternating sequence of working memory tasks, such that a location task was initiated immediately upon the end of the response interval for the preceding shape task. Each subject was given two practice runs prior to entering the magnet, followed by two practice runs in the magnet. The testing session consisted of a total of 6–8 runs, each comprising 20 (Exp1A) or 18 (Exp1B) task cycles and lasting 198 sec, which included 174.6 sec of alternating tasks plus no-task baseline periods preceding and following the tasks (23.8 sec). Task order was changed across imaging runs such that one run started with the shape task (SLSL . . .), and the next run started with the location task (LSLS . . .).

Experiment 2 tasks

In experiment 2, subjects performed a continuous series of tasks within a single processing domain (spatial or object) which alternated between a working memory task and a nonmemory perceptual control. In four runs, shape working memory alternated with shape perceptual control. In the remaining four runs, location working memory alternated with location perceptual control. As in experiment 1, the starting task within a domain varied such that one run started with the working memory task and the next run started with the perceptual control task.

The location and shape working memory tasks were the same as used in experiment 1. The location perceptual control task was structured similarly to the working memory task, except that the three white squares appearing at random locations on the screen remained visible throughout the entire 3.5-sec former retention delay interval. A red target square appeared during the response period, which overwrote one of the three white squares on half of the trials. To indicate when a prior location had been overwritten, the red target square was slightly smaller than the underlying white square. On the remaining half of the trials, the red

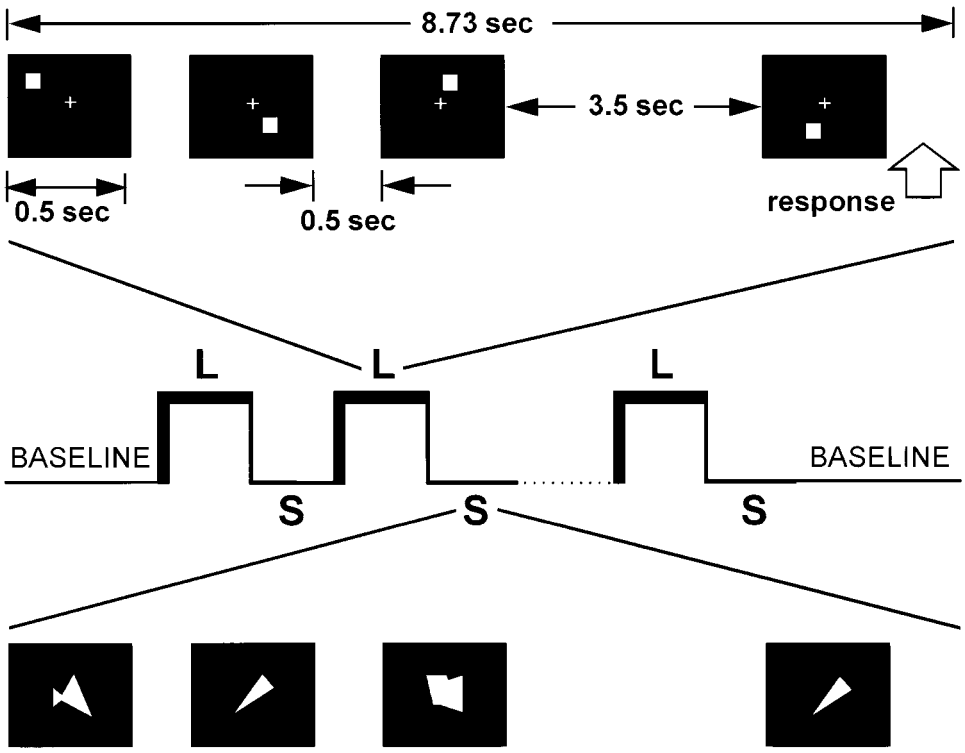

Figure 1.

Schematic illustration of the alternating location and shape working memory tasks used in experiment 1. Each task had a duration of 8.73 sec, during which each of three white test stimuli was presented for 0.5 sec with a 0.5-sec interstimulus interval (ISI). Following the third test stimulus, a 3.5-sec delay period occurred during which the subject fixated a central cross. A red target stimulus was then presented which matched one of the test stimuli on half of the trials. The subject was instructed to press one of two buttons with their right hand to signal whether the target matched or did not match any of the preceding three test stimuli (open arrow). The expanded view of one location (L) memory task cycle (top) shows a trial in which the target is a nonmatch, whereas the shape (S) working memory task cycle (bottom) shows a target matched to one of the test stimuli. In experiment 1A, the 10 alternations of the location and shape tasks were preceded and followed by a 7-sec no-task baseline period. In experiment 1B, nine alternations of the location and shape tasks were used, with an extended baseline period of 17.46 sec.

target appeared in a new location. The subject compared the location of the red square to the still visible white squares to determine whether the location of the target matched that of any of the three white squares.

In the shape perceptual control task, sections of the complex polygons generated in the working memory condition appeared successively at the center of the screen, such that the final complete shape was unveiled in three stages corresponding to the timing intervals of the working memory task. When the final shape was completed at the third stage it remained on the screen during the 3.5-sec interval until the red target shape appeared. On half of the trials, the red target completely overwrote the white shape and the subject responded that the target shape matched. On the nonmatching half of the trials, the white and red shapes did not match. Thus, neither the shape nor location perceptual control tasks had any significant memory component. Again, during all tasks, subjects were instructed to maintain central fixation.

For both experiments, timing and stimulus presentation were controlled by computer. Stimuli were back-projected from an active matrix LCD projection panel (Sharp QA 1150) using an overhead projector (3M 955) upon a translucent Plexiglas screen mounted on the patient gurney. The visible display area subtended 14.5° (horizontal) by 10.9° (vertical) of visual angle. The subject viewed the screen from a mirror mounted on the head coil.

The two-task alternation design used in experiments 1 and 2 emphasizes regions *differentially* activated by each task. Thus, the alternation of the shape and location working memory tasks in experiment 1 is expected to reveal anatomical regions differentially activated by the two processing domains. These activations will include any regions supporting domain-

specific working memory as well as regions supporting domain-specific perceptual processing. In contrast, the within-domain alternation between working memory and perceptual control tasks in experiment 2 will reveal regions differentially activated by the cognitive demands imposed by working memory, whether specific or nonspecific to a processing domain.

MR image acquisition

In order to acquire more slices than was technically feasible in a single session on our imaging system, experiment 1 was divided into two sessions. Four slices were acquired through the prefrontal cortex in experiment 1A, and seven slices through the posterior brain in experiment 1B. In experiment 2, seven slices were imaged: two through the prefrontal cortex and five through the posterior brain. The slice selection of experiment 2 was guided by the results of experiment 1 and is illustrated in Figure 2.

Images were acquired on a 1.5 Tesla General Electric (Milwaukee, WI) Signa MRI scanner equipped with a quadrature headcoil and an Advanced NMR Instascan (Wilmington, MA) echoplanar imaging subsystem. The subject's head was immobilized using a vacuum cushion and forehead and chin straps. Each imaging session started with the acquisition of T1-weighted sagittal anatomical localizers (TR = 500 msec, TE = 11 msec, NEX = 1, FOV = 24 cm, matrix = 128 × 128, slice thickness = 5 mm, skip = 2.5 mm) to identify the anterior and posterior commissures. For experiment 1A, four coronal slices were selected centered 35 mm anterior to the anterior commissure (Fig. 2). T1-weighted (TR = 500 msec, TE = 11 msec, NEX = 2, FOV = 40 cm, matrix = 256 × 192, slice thickness = 7 mm, skip = 0 mm) images of these slices were acquired for later anatomical coregistration. The anterior-posterior (Y) Talairach coordinates of the four planes were approximately F1 = +42 mm, F2 = +38.5 mm, F3 = +31.5 mm, and F4 = +24.5 mm. For experiment 1B, seven coronal slices were selected, beginning 15 mm posterior to the anterior commissure (Fig. 2). The anterior-posterior (Y) Talairach coordinates of the seven slices were approximately P1 = −15 mm, P2 = −24 mm, P3 = −33 mm, P4 = −42 mm, P5 = −51 mm, P6 = −60 mm, and P7 = −69 mm. For experiment 2, the functional imaging sequence was changed so that the adjacent 7-mm-thick slices were separated by a 2-mm skip. Slice selection was therefore adjusted so that the two frontal slices were centered 30 mm anterior to the anterior commissure and matched F3 and F4 of experiment 1A (Fig. 2). The five posterior slices were selected beginning 33 mm posterior to the posterior commissure and matched posterior slices P3–P7 of experiment 1B (Fig. 2).

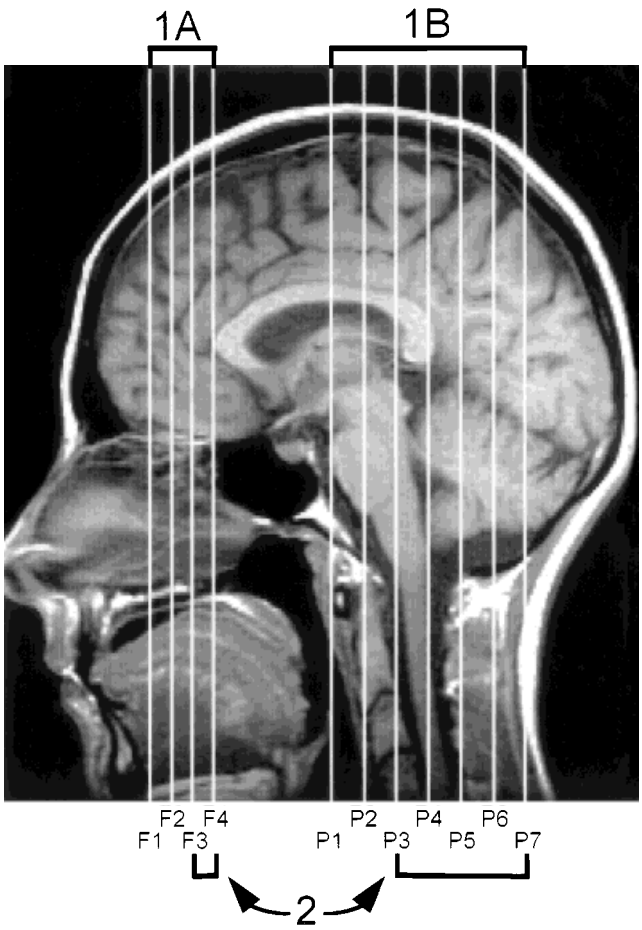

Figure 2.
Coronal slice selection for experiments 1 and 2. In experiment 1A, four frontal slices (F1–F4) were imaged at the following average Talairach anterior-posterior (Y) coordinates: F1 = +45.0, F2 = +38.5, F3 = +31.5, and F4 = +24.5. In experiment 1B, seven posterior slices (P1–P7) were imaged at the following average Talairach y coordinates: P1 = −15, P2 = −24, P3 = −33, P4 = −42, P5 = −51, P6 = −60, and P7 = −69. Seven slices were imaged during experiment 2, approximately matching slices F3, F4, and P3–P7 in experiment 1.

Functional images were acquired using a gradient echo echoplanar (EPI) pulse sequence (TR = 1.5 sec, TE = 45 msec, α = 60°, NEX = 1, FOV = 20 × 40 cm, matrix = 128 × 64, slice thickness = 7 mm, skip = 0 mm). Each experimental run consisted of 128 EPIs per slice at the TR interval of 1.5 sec, yielding a 196-sec scan time. Each run was preceded by 4 RF excitations per slice to achieve steady-state transverse magnetization. The first experimental task commenced 7 sec after acquisition of the first image.

Following the acquisition of functional image series, a series of whole-brain axial spoiled grass (SPGR) images (TR = 25 msec, TE = 5 msec, FOV = 24 cm, $\alpha = 45°$, slice thickness = 2 mm, skip = 0 mm) was acquired for each subject. Coronal magnetic resonance angiograms (TR = 45 msec, TE = 7.7 msec, FOV = 24 cm, $\alpha = 40°$, slice thickness = 2 mm, skip = 0 mm) were acquired to examine contributions from major venous vasculature.

Image analysis

Activations were identified by the construction of individual and group t-maps. In addition, a frequency analysis was performed to identify the number and anatomical location of voxels activated by each task. These methods have been presented in detail in McCarthy et al. [1995] and Puce et al. [1995, 1996] and are briefly summarized here. For the construction of the t-maps, the four (or three) runs for each stimulus alternation order were averaged. For example, in experiment 1 this resulted in one average run of 128 images per slice for the location-shape task order (LSLS . . .) and one average run per slice for the shape-location task order (SLSL . . .). Three consecutive images were selected from each cycle for each task. In experiments 1A and 2, there were 10 task cycles per run, resulting in 30 images per task for analysis, while in experiment 1B, there were nine task cycles per run resulting in 27 images per task. An unpaired t-test was then performed on a voxel-by-voxel basis for these images. Because the fMRI activation signal typically reaches its peak level 4–6 sec after task onset, the three consecutive images chosen for t-test analysis were those beginning 6.5 sec after task onset. A compensation in this selection was introduced to account for the offset within each TR for the acquisition of individual slices. The resulting two t-maps for each slice were examined for consistency, and average-t maps [Puce et al., 1996] were generated for each subject.

Translation, rotation, and stretch factors were determined to transform each subject's high-resolution anatomical images onto a reference brain, resulting in the generation of a series of average brain slices. These transformation factors were determined without reference to functional data, and were performed separately for each hemisphere to avoid bias and to improve accuracy. To match the individuals' anatomical and functional images to the reference anatomical image, it was sometimes necessary to offset the slice order of the functional and anatomical image in individual subjects to match the reference images (e.g., slices P2–P6 from one subject might be aligned with reference slices P1–P5). Group activation t-maps were then computed and superimposed upon the average anatomical slices.

The frequency domain analysis consisted of a fast Fourier transform of the 128 sample time series of each voxel to identify those voxels showing periodic MR signal changes at the task alternation frequency. Voxels were retained in which the spectral power at 0.057 Hz (corresponding to the two-task alternation period of 17.46 sec) was greater than 1.5 standard deviations from the mean power at the 14 adjacent spectral estimates. A second stage of processing examined the relative phases of the activation signal for these significant voxels. Because runs differed in the starting task (i.e., S-L or L-S), activation signals from voxels evoked by a particular task varied in phase by approximately 180° between each run pair. Thus, activated voxels were defined as those in which significant power was obtained for both run pairs, *and* in which the relative phases changed by $180 \pm 15°$ between run pairs.

Figure 3 illustrates these analyses in an individual subject, using a region of activation in the left occipito-temporal sulcus (OTS) during the shape working memory task in experiment 1B. The time course of activation for the activated voxels in the left OTS (Fig. 3A, white square) showed a periodic signal change whose rise was synchronized to the onset of the shape task (Fig. 3B). The two curves correspond to the two alternation orders, and reflect the 180° phase shift due to task presentation order. The peaks correspond to the nine shape tasks presented during the run. The frequency analysis shows the greatest power at 0.057 Hz, corresponding to the task alternation frequency (Fig. 3C, arrow). The phase analysis reveals that the relative phases of voxels activated at 0.057 Hz showed a 180° phase shift between alternation orders (Fig. 3D). The anatomical location [Duvernoy, 1991] and the Talairach coordinate [Talairach and Tournoux, 1988] of each activated voxel were determined. The locations of activation were compared to regions predicted on the basis of previous imaging studies [McCarthy et al., 1994, 1996].

RESULTS

Experiment 1

Behavioral results

A t-test was performed on the accuracy of subjects' responses to determine whether the two working memory tasks differed in difficulty. The mean accuracy for the location working memory task averaged across

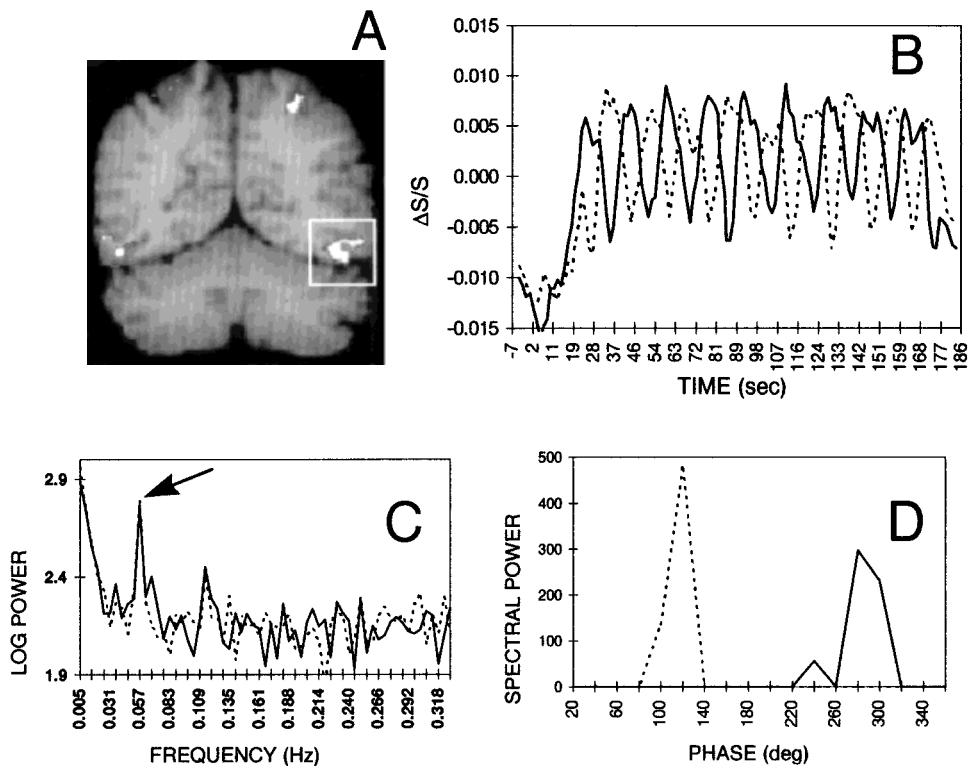

Figure 3.

fMRI activation data for the shape working memory tasks used in experiment 1 from an individual subject. **A:** Average t-test data for slice P6 overlaid on a corresponding T1-weighted anatomical image. In this and all subsequent figures the right side of the brain appears on the left side of the image. The temporal characteristics for the highlighted activation in the left occipitotemporal sulcus (white square) are displayed in B–D. **B:** Time course of activation for reference region. The two curves represent the S-L alternation order (solid line) and L-S alternation order (broken line). Signal change (ΔS/S) is represented on the y-axis. Task onset occurred at 17 sec, and task offset occurred at approximately 174 sec. Note the nine peaks which match the nine task alternation cycles. The change in task order produced a 180° shift in the waveform. **C:** Power spectral data (logarithmic scale) from the region of interest shown in A. Note the peak at the task alternation frequency at 0.057 Hz (arrow) for both task orders. **D:** Power at the task alternation frequency as a function of phase shows two peaks for the two task orders, separated by approximately 180°.

experiments 1A and 1B (mean = 76.24%, SD = 14.88) was slightly greater than for the shape working memory task (mean = 70.11%, SD = 14.30) ($t(15) = 1.75$, $P < 0.01$). During debriefing, most subjects reported that the shape task was more difficult due to the highly abstract nature of the computer-generated polygons, which hampered their ability to use verbal labeling strategies. The implications of differences in task difficulty for interpretation of the results will be discussed later.

Activation results

Figure 4 compares activations in 6 representative individuals (Fig. 4A–F) for the shape (Fig. $4A_S$–F_S) and location (Fig. $4A_L$–F_L) working memory tasks, in frontal (Fig. 4A–C) and posterior (Fig. 4D–F) slices. There were three major findings. First, in anterior frontal regions (Fig. 4A), strong left middle frontal gyrus (MFG) activation was obtained for shape working memory (Fig. $4A_S$). Second, shape working memory showed a more bilateral pattern of MFG activation in the more posterior frontal slice, as can be seen for two additional individuals (Fig. $4B_S$, C_S). Finally, no activation was observed in MFG for the location working memory task in these individuals (Fig. $4A_L$–C_L), although some activation of the superior frontal gyrus (SFG) was observed in one subject (Fig. $4B_L$). The lack of MFG activation observed for location working memory was expected on the basis of prior findings by McCarthy et al. [1996], which demonstrated that location working memory primarily activated the right MFG. As this same region was also activated by shape

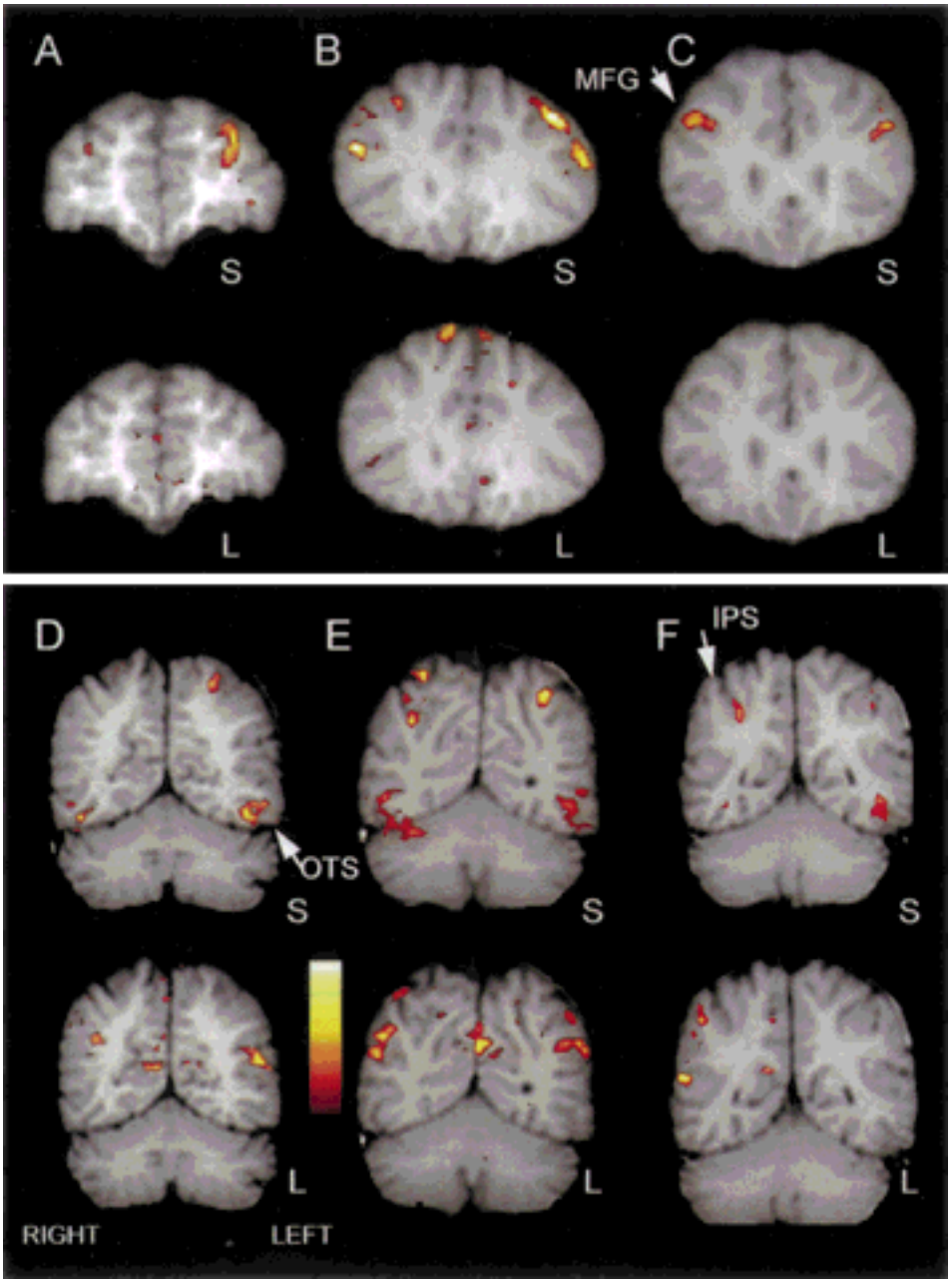

Figure 4.

Representative data from 6 individual subjects for the shape and location working memory tasks. Each image represents the results of the t-test analysis for that individual superimposed upon a T1-weighted anatomical image. **A_S–C_S:** Results from shape working memory for 3 individuals in experiment 1A. **A_L–C_L:** Corresponding location working memory data for the same subjects and slice as shown in A_S–C_S (anterior-posterior (Y) Talairach coordinate A = +42 mm, B = +24.5 mm, and C = +24.5 mm). **D_S–F_S:** Results from shape working memory for 3 individuals in experiment 1B. **D_L–F_L:** Corresponding location working memory data for the same subjects and slices as shown in D_S–F_S.

working memory in the prior study, the present alternating design additionally indicated that dPFC activation by location working memory partially overlapped the activation evoked by shape working memory.

Figure 4 also depicts the consistency of the activation patterns in posterior regions (Fig. 4D–F). In the posterior slices, the shape working memory task activated the intraparietal sulcus (IPS) and OTS bilaterally

(Fig. 4D_S–F_S), particularly in the left hemisphere. In the same 3 subjects, location working memory task activated the angular gyrus (predominantly in the left hemisphere), the IPS, and the precuneus (PC) (Fig. 4D_L–F_L).

Across-subject results are depicted in Figures 5 and 6, which present the group-averaged t-maps for the location and shape working memory tasks, respectively. Location working memory activated portions of the frontal lobes, principally the medial aspect of the SFG and anterior cingulate gyrus (ACG) (Fig. 5, slices F1 and F2). Consistent with the results in individual subjects, posterior activation was observed in the inferior parietal lobe including the angular gyrus (AG) (P5–P7), and the midline cortex from the posterior cingulate to the parieto-occipital fissure (P4–P7). In contrast, shape working memory (Fig. 6) activated left prefrontal regions at F1 and F2 with strong bilateral activation of the MFG at F4, again highly consistent with individual data. In the posterior cortex, extensive activation of the IPS was observed (P3–P7), with greater activation occurring in the left hemisphere. Intense bilateral activation of the OTS and inferior temporal sulci (ITS) (P5–P7) and the fusiform gyri (FG) (P4–P5) was also observed.

To quantify the distribution of activation during the location and shape working memory tasks, the activated voxels identified in the frequency domain analysis from each subject were tabulated by anatomical region and hemisphere (Fig. 7). In addition, the mean Talairach coordinates for each activated region are presented in Table I. In the frontal lobe, location (Fig. 7A) activated a greater number of voxels in the SFG relative to shape (Fig. 7B). As shown in Table I, this activation was centered on the medial aspect of the SFG. The shape working memory task yielded greater activation of the dPFC, primarily confined to the middle and inferior frontal gyri (IFG). In posterior regions, shape strongly activated the IOTC (Fig. 7B), which comprised the OTS, FG, and ITS. In contrast, the AG, posterior cingulate gyrus (PCG), and PC were almost exclusively activated by the location working memory task. The supramarginal gyrus (SMG), parallel sulcus (PS), and IPS were partially activated by both working memory tasks. Comparing hemispheres, shape activated the left hemisphere to a greater extent than the right, particularly in the OTS and IPS. Location presented a more mixed hemispheric pattern, with stronger activation of the right IPS and SFG (Fig. 7).

In summary, experiment 1 demonstrated a different pattern of activation for spatial and object processing domains during the performance of similarly structured working memory tasks. Shape working memory differentially activated the MFG bilaterally, and the IFG in the left hemisphere. Also differentially activated were the OTS and FG. Location working memory primarily activated the medial aspect of the SFG and ACG anteriorly, and the AG, PCG, and PC posteriorly. The greater ventral activation for shape and dorsal activation for location agrees with prior studies, which argued for the existence of two visual pathways: a ventral pathway for visual feature extraction, and a dorsal pathway for locating objects in space [Ungerleider and Mishkin, 1982].

The areas activated in experiment 1 were differentiated on the basis of processing domain *within* the context of a working memory task. Thus, regions activated in common by both working memory tasks, independent of domain, should show little or no activation. For example, McCarthy et al. [1996] reported that shape working memory activated the MFG bilaterally and the left IFG, consistent with the results reported here. In their study, location working memory also strongly activated the right MFG, but only weakly activated the left MFG. In the present study, the common activation of the right MFG by location was not observed, as predicted by the alternating design.

Experiment 2

Experiment 2 was conducted to determine which of the activations obtained in experiment 1 were specific to working memory and not to the processing domain per se, and to identify regions which were commonly activated by working memory independent of processing domain. As one subject in this experiment did not show any activation, all analyses were performed on 11 subjects.

Behavioral results

An analysis of variance performed on subjects' response accuracy showed a significant task effect ($F(3, 43) = 20.69$, $P < 0.0001$). Post hoc pairwise comparisons indicated that subjects were more accurate for both perceptual controls than working memory tasks ($P < 0.0001$ for both shape and location). As in experiment 1, more errors occurred for shape than for location working memory ($P < 0.05$). There was no significant difference between shape and location perceptual control conditions.

Activation results

Figure 8A, B depicts the group-averaged t-maps during the location working memory and location

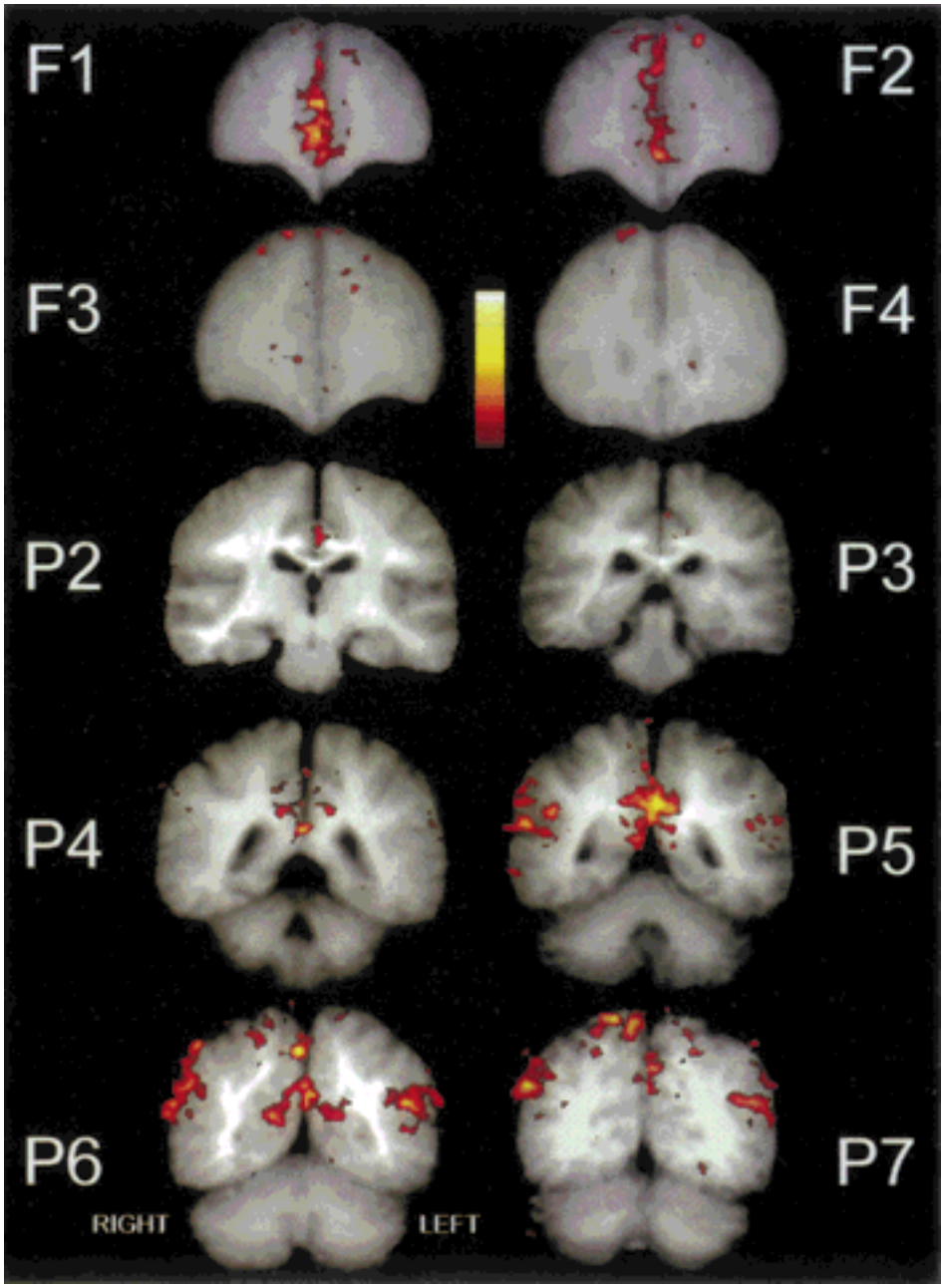

Figure 5.
Experiment 1. Average group activation t-maps for the location working memory task superimposed upon average anatomical MRIs for four frontal (F1–F4) and six posterior (P2–P7) coronal slices. No significant activation occurred in posterior slice P1 (not shown). Higher t-values are shown by the yellow-white end of the color scale in this and subsequent figures.

perceptual control task, respectively. Figure 9A, B depicts the group-averaged t-maps during the shape working memory and shape perceptual control task, respectively. Compared to the location perceptual task, location working memory strongly activated the right MFG, with lesser activation of the anterior cingulate cortex (F4, Fig. 8A). Shape working memory differentially activated the MFG in the right hemisphere and the MFG and IFG in the left hemisphere (F3–F4, Fig. 9A). Weak activation of the anterior cingulate region

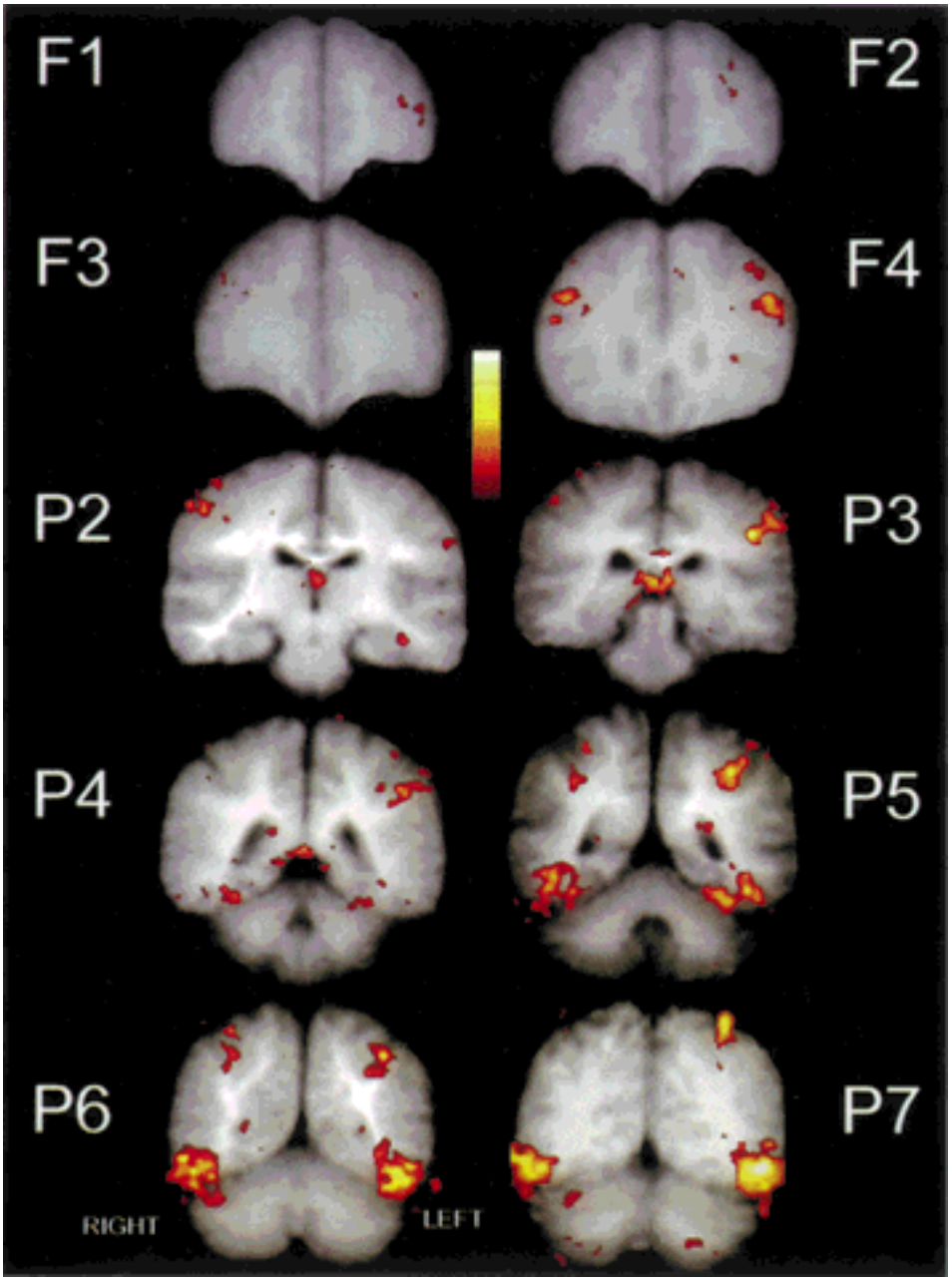

Figure 6.
Experiment 1. Average group activation t-maps for the shape working memory task superimposed upon average anatomical MRIs for four frontal (F1–F4) and six posterior (P2–P7) coronal slices. No significant activation occurred in posterior slice P1 (not shown).

was also detected for both working memory tasks (F4, Figs. 8A, 9A). No significant PFC activation was obtained for either the location or shape perceptual control tasks (Fig. 8B, F3–F4, Fig. 9B, F3–F4, respectively).

The pattern of activation for individual subjects in the PFC was consistent with these group-averaged results. The t-maps from the shape working memory task for individual subjects showed prefrontal activation in 9 of 11 subjects. In 3 of these 9, the activation occurred unilaterally in the left prefrontal cortex, while the remaining 6 activated bilaterally. In 3 of these 6, the left hemisphere activation extended inferiorly from the MFG to the IFG. In contrast to shape working memory,

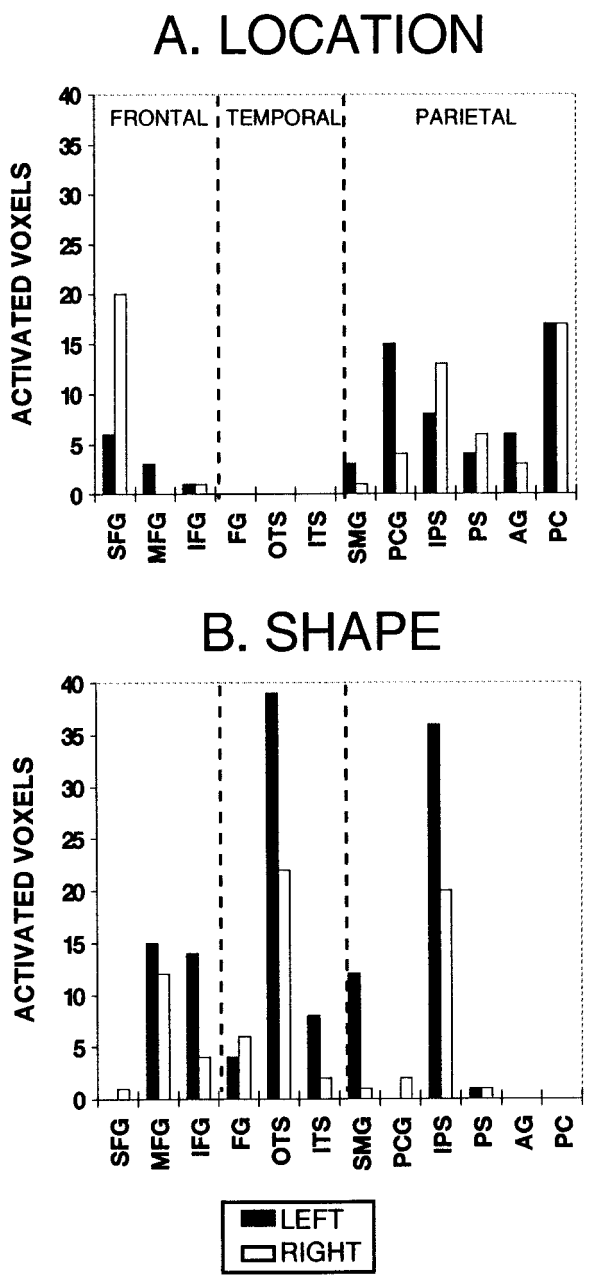

Figure 7.

Experiment 1. Number and anatomical distribution of activated voxels within the frontal, parietal, and temporal lobes as a function of left and right hemispheres. **A:** Location working memory task. **B:** Shape working memory task. SFG, superior frontal gyrus; MFG, middle frontal gyrus; IFG, inferior frontal gyrus; FG, fusiform gyrus; OTS, occipitotemporal sulcus; ITS, inferior temporal sulcus; SMG, supramarginal gyrus; PCG, posterior cingulate gyrus; IPS, intraparietal sulcus; PS, parallel sulcus; AG, angular gyrus; PC, precuneus.

the location working memory task activated the right MFG exclusively.

In the parietal lobe, location working memory activated the right IPS in slice P4, and the IPS bilaterally in slices P5–P7 (Fig. 8A). Unlike experiment 1, no activations were observed in the AG and SMG. Compared to its perceptual control, shape working memory presented a strikingly similar activation pattern as location working memory when compared to its perceptual control (compare Figs. 8A and 9A). The IPS was strongly activated, particularly in the left hemisphere

TABLE I. Number (N) and anatomical location (in Talairach coordinates) of activated voxels in experiment 1 for the shape and location working memory tasks*

Anatomical location	N	X	Y	Z
Shape				
SFG (R)	1	21	50	35
SFG (L)	0			
MFG (R)	12	30	34	37
MFG (L)	15	−33	33	24
IFG (R)	4	42	34	12
IFG (L)	14	−36	31	10
FG (R)	6	32	−53	−15
FG (L)	4	−36	−54	−18
OTS (R)	22	43	−54	−10
OTS (L)	39	−43	−54	−15
ITS (L)	8	−54	−57	−6
SMG (L)	12	−57	−33	30
IPS (R)	20	28	−52	41
IPS (L)	36	−35	−55	35
Location				
Med SFG (R)	20	5	45	7
Med SFG (L)	6	−2	47	13
MFG (R)	0			
MFG (L)	3	−22	32	16
IFG (R)	1	46	33	12
IFG (L)	1	−24	42	−11
PC (R)	17	6	−53	35
PC (L)	17	−5	−54	38
PCG (R)	4	2	−41	33
PCG (L)	15	5	−39	28
PS (R)	6	47	−48	21
PS (L)	4	−57	−40	−2
AG (R)	3	44	−57	33
AG (L)	6	−51	−61	18
IPS (R)	13	28	−52	46
IPS (L)	8	−29	−62	43

*SFG, superior frontal gyrus; MFG, middle frontal gyrus; IFG, inferior frontal gyrus; FG, fusiform gyrus; OTS, occipitotemporal sulcus; ITS, inferior temporal sulcus; SMG, supramarginal gyrus; PCG, posterior cingulate gyrus; IPS, intraparietal sulcus; PS, parallel sulcus; AG, angular gyrus; PC, precuneus.

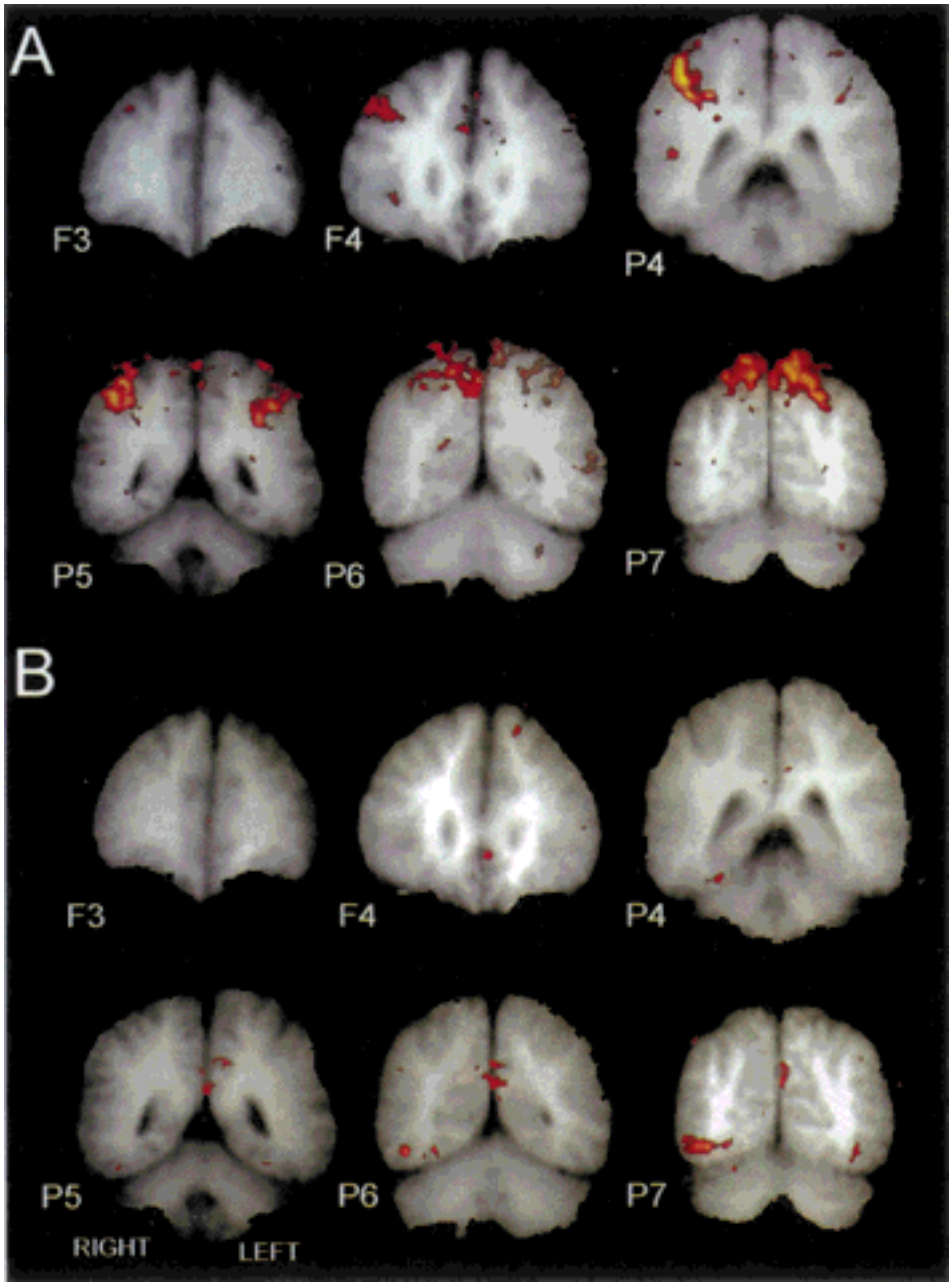

Figure 8.
Experiment 2. Average group t-maps for frontal (F3, F4) and posterior brain regions (P4–P7) for the location processing domain. **A:** Working memory task. **B:** Perceptual control task.

(e.g., P4–P6, Fig. 9A). Like that of the dPFC, the IPS activation was only obtained during the working memory tasks and not the perceptual control tasks (Figs. 8B, 9B). The shape-related IOTC activations which dominated experiment 1 were greatly diminished in experiment 2, with only a small region remaining in the left hemisphere (P7, Fig. 9A).

To evaluate the relative specificity of the activations for domain and task in the posterior brain, a comparison of the number of activated voxels in the IPS and IOTC was performed for the working memory tasks for experiments 1 and 2. Figure 10 presents the number of activated voxels derived from the frequency domain analysis for shape and location working memory. For

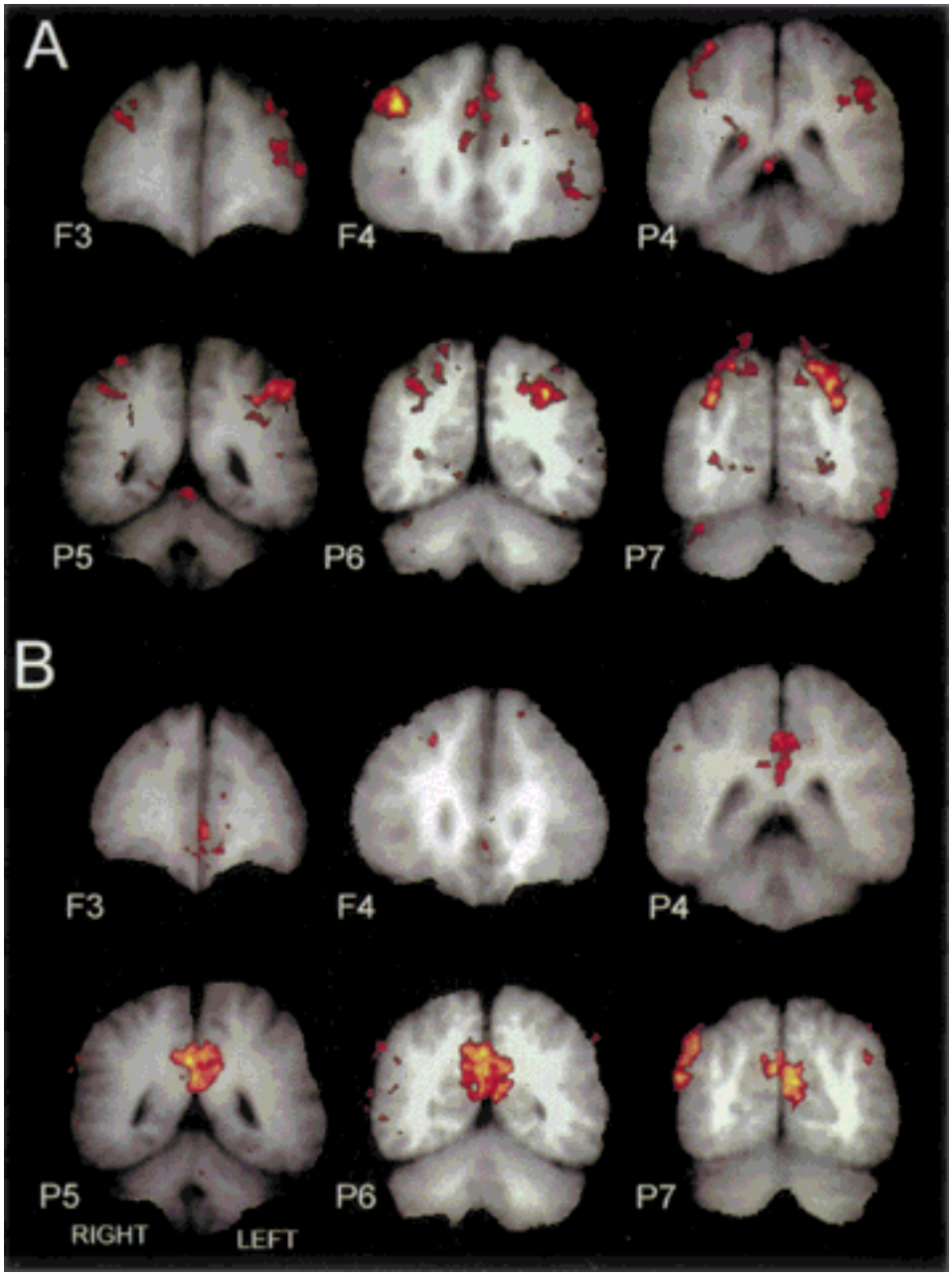

Figure 9.
Experiment 2. Average group t-maps for frontal (F3, F4) and posterior brain regions (P4–P7) for the shape processing domain. **A:** Working memory task. **B:** Perceptual control task.

shape working memory, 78 voxels were obtained in the IOTC in experiment 1, but only 17 voxels in experiment 2. Thus, the majority of activated voxels were obtained when alternating perceptual domains, but not when alternating perceptual and mnemonic object processing.

The voxel count within the IPS increased for both shape and location working memory when compared to their respective perceptual controls, and the increase was largest for the location task. These results suggest that the IPS activation was driven in part by the demands of the working memory task, and that there was a partial overlap in the activations for the shape and location tasks. These common activations were masked when the working memory tasks were alternated with each other. Shape working memory strongly

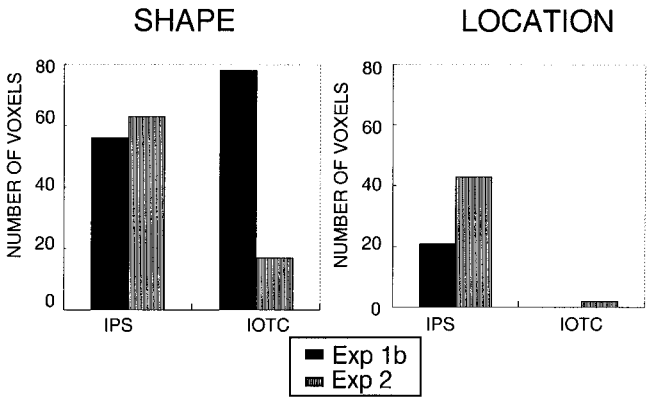

Figure 10.
Experiments 1B and 2. Number and anatomical distribution of voxels activated during the shape and location working memory tasks in the intraparietal sulcus (IPS) and the inferior occipitotemporal cortex (IOTC). This latter region summed voxels from the fusiform gyrus and occipitotemporal sulcus.

activated the IPS in both experiments; however, shape activation was greater in the left IPS in experiment 1, while location activation was greater in the right IPS (Fig. 7). Thus, the hemispheric pattern of activation for the IPS for working memory paralleled that of the dPFC.

Midline and PCG activation was observed for both perceptual control tasks, with much stronger activation during the shape perceptual task (Fig. 9B). The time courses of activation in the PCG and IPS were examined for the shape working memory and shape perceptual control task by computing an average task cycle representing the average of nine task cycles for each of four runs (Fig. 11). The activation in the IPS peaked at the end of the working memory task. The activation of the PCG showed a reciprocal pattern in which the activation peaked at the conclusion of the perceptual control task.

DISCUSSION

The present experiments showed that mnemonic and perceptual components of spatial and nonspatial working memory tasks activated distinct regions in parietal, temporal, and prefrontal cortices. The differential contributions of domain (spatial vs. nonspatial) and task (mnemonic vs. perceptual) specific activations at each of these anatomical foci will be discussed below.

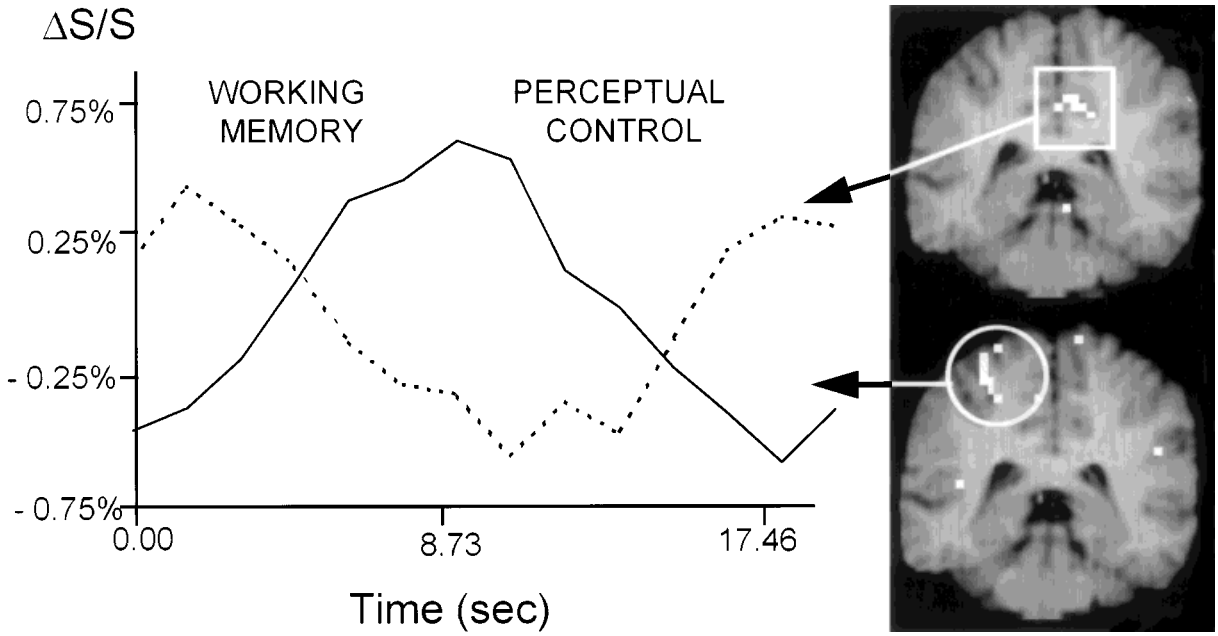

Figure 11.
Experiment 2. Single task cycle (averaged over nine cycles) in the posterior cingulate (top right image, white square) and intraparietal sulcus (bottom right image, white circle) during the shape working memory and perceptual control tasks for an individual subject. Solid line represents activation in the intraparietal sulcus, and broken line represents activation in the posterior cingulate.

Parietal cortex

Two regions of the parietal cortex showed different degrees of domain and task specificity. The inferior parietal cortex, principally the AG, was activated by location working memory when alternated with shape working memory, but not when alternated with the location perceptual task. Thus, like the IOTC, this region showed strong domain specificity. The second region, the IPS, showed a more complex pattern of activation. When alternated, both working memory tasks activated the right IPS, and the shape task also activated the left IPS. The number of activated voxels in the IPS increased for *both* working memory tasks but particularly for location when compared with the respective perceptual controls. This suggests that part of the IPS activation was independent of perceptual domain and was driven by common cognitive demands of the working memory tasks.

Nonhuman primate studies have demonstrated a strong anatomical [Cavada and Goldman-Rakic, 1989; Selemon and Goldman-Rakic, 1988] and functional [Friedman and Goldman-Rakic, 1994; Goldman-Rakic et al., 1993; Goldman-Rakic and Chafee, 1994] link between the dorsolateral prefrontal and posterior parietal regions during spatial working memory tasks. Physiological evidence suggests that the IPS is sensitive to eye movements [Duhamel et al., 1992], oculocentric coordinates, position of gaze, and the direction, speed, and distance of visual stimuli [Colby et al., 1993, 1995], and is engaged in the encoding of spatial location and processing of spatial relations [Andersen, 1995; Colby et al., 1995]. The present results extend these findings by demonstrating activation of the IPS in spatial working memory. However, the activation of the IPS by the shape working memory is surprising, given the segregation of function between the dorsal and ventral visual pathways. Relevant here are the reciprocal anatomical connections between the IPS and IOTC reported in nonhuman primates [Distler et al., 1993], which may play a role in the activation of the IPS during shape working memory.

Inferior occipitotemporal cortex

The strong differential activation of the inferior occipitotemporal cortex by shape working memory in experiment 1B (Fig. 6) is consistent with the role of the ventral visual pathway in feature analysis [e.g., Ungerleider and Mishkin, 1982]. The significant decrease in the activation of the left IOTC by shape working memory relative to its perceptual control suggests that this activation was largely driven by the perceptual component of both tasks (Fig. 9). However, since a small proportion of voxels was still activated when shape working memory was compared to its perceptual control, a role for this region in working memory cannot be excluded. This is consistent with physiological studies demonstrating activity in the IOTC during both perceptual processing and, to a lesser extent, during delay-intervals, suggesting that this region mediates not only the recognition of object features, but also their learning and retention [Lueschow et al., 1994; Miller and Desimone, 1994; Fuster and Jervey, 1982].

Anterior and posterior midline cortex

Activation patterns for the anterior and posterior midline cortices were complex. The posterior midline cortex, which comprises the PCG and PC, showed strong activation during location working memory when alternated with shape working memory (P4–P7, Fig. 5), for shape perceptual control when alternated with shape working memory (P4–P6, Fig. 9B), and, to a lesser degree, for location perceptual control when alternated with location working memory (P5–P7, Fig. 8B). Since this region showed no activation for either working memory task when compared to the perceptual controls, it is unlikely that the demands of working memory per se activated this region. However, it is possible that activity in the posterior midline cortex was synchronized to the end of the working memory tasks and appeared in the alternate task cycle. The activation in the anterior midline cortex, which here primarily included the medial aspect of the SFG and to a lesser extent the anterior cingulate cortex, showed a similar peak at the end of the task cycle. Similar posttask activation for the frontal midline cortex was seen by McCarthy et al. [1996] and was greatest following shape working memory. As discussed above, the strong midline activation for location working memory (Fig. 5, F1, F2) is also consistent with McCarthy et al. [1996].

The functional role of the anterior and posterior cingulate cortices are unclear. Neuroimaging studies have implicated the anterior portions in working memory [McCarthy et al., 1996], selective attention [Posner et al., 1987; Pardo et al., 1990], and sustained attention [Grossman et al., 1992]. Lesions to the posterior cingulum bundle and retrosplenial region have been reported to yield amnesia, even in the absence of hippocampal, thalamic, or other limbic structure involvement [Heilman and Sypert, 1977; Valenstien et

al., 1987]. A recent review by Sutherland and Hoesing [1993] reported that the posterior cingulate cortex, around Brodman's area 29, is implicated in spatial memory, such that lesions to this region have effects similar to those of hippocampal lesions upon navigation and maze learning. In the present study, the posterior cingulate may have been inhibited during the working memory task interval and released at task offset. Thus, the posttask activation may represent a return to baseline. However, the posttask anterior cingulate activation found by McCarthy et al. [1996] occurred relative to a nontask baseline, suggesting its relationship to posttask decision processes. These issues will require further study, using an experimental design which does not confound the posttask interval with a competing task.

Prefrontal cortex

Activation of the PFC, particularly the MFG, was task-specific in that it was differentially activated by the working memory tasks when compared to their nonmemory perceptual controls. This result confirms prior studies from our group [McCarthy et al., 1994, 1996] and others [e.g., Petrides et al., 1993a,b; Cohen et al., 1994; Swartz et al., 1994; Smith et al., 1995, 1996; see review by McCarthy, 1995]. McCarthy et al. [1994, 1996] previously demonstrated that nonmemory, but attention-demanding, tasks also activated the MFG, but at about half the level of working memory tasks. Unless activation of dPFC by the perceptual tasks exceeded that for working memory, or had a distinct anatomical locus, it would not be observed using the alternating design. Therefore, the lack of dPFC activation by the perceptual tasks here (Figs. 8B, 9B) is consistent with these prior results.

Domain specificity for working memory in dPFC was demonstrated by hemispheric differences in activation. Shape working memory activated the MFG bilaterally. In some subjects, the activation extended into the left IFG, in agreement with Wilson et al. [1993], who found that neurons in ventral regions of the prefrontal cortex were selectively activated during nonspatial working memory tasks. When compared to its perceptual control, location working memory activated the right MFG. However, the absence of MFG activation by location working memory in experiment 1A suggests that right MFG activation was common to both working memory tasks, consistent with previous studies [McCarthy et al., 1996; Baker et al., 1996; Smith et al., 1996]. At the most posterior frontal slice, shape and location working memory activated the right MFG to the same anatomical extent when compared to their respective perceptual controls (compare Figs. 8B and 9B, slice F4). However, the higher t-values for the shape task resulted in bilateral MFG activation when shape and location working memories were alternated. As shape working memory was more difficult, this stronger activation of the right MFG should be interpreted cautiously, as task difficulty may confound quantitative comparisons.

In addition to the dPFC, activation of the medial aspect of the SFG by location working memory was observed in the most anterior slices (Fig. 5, F1, F2). This region was not strongly activated in our prior studies [McCarthy et al., 1994, 1996]. As F1–F2 were not acquired in experiment 2, additional experiments will be necessary to determine whether these activations were evoked by location working memory per se.

Network for working memory

Our findings suggest the existence of parallel cortical networks distributed within the right and left hemispheres supporting spatial and nonspatial working memory, respectively. The frontal regions participated primarily in the mnemonic aspect of working memory, while the posterior parietal regions processed both the perceptual and the mnemonic aspects of the tasks. In contrast, the inferior temporal cortex was largely unaffected by the additional demands of working memory and therefore appeared to be involved primarily with perceptual processing. As demonstrated by the shape task, most cognitive operations probably access both hemispheric networks. The interplay between frontal and posterior regions in maintaining sensory information on-line, and the manner in which the hemispheric networks are integrated in processing multidomain stimuli, require further study.

ACKNOWLEDGMENTS

This work was supported by the Department of Veterans Affairs, in aid to the Schizophrenia Biological Research Center and the VA-Yale Alcoholism Research Center, and by NIMH grants MH-44866 and MH-05286. We thank Marie Luby, Hedy Sarofin, Francis Favorini, and Charlotte Bayat for assistance.

REFERENCES

Andersen RA (1995): Encoding of intention and spatial location in the posterior parietal cortex. Cereb Cortex 5:457–469.

Baddeley A (1986): Working Memory, Oxford: Clarendon.

Baker SC, Frith CD, Frackowiak RS, Roland RJ (1996): Active representation of shape and spatial location in man. Cereb Cortex 6:612–619.

Barbas H (1988): Anatomic organization of basoventral and mediodorsal visual recipient prefrontal regions in the rhesus monkey. J Comp Neurol 276:313–342.

Barbas H, Mesulam M-M (1981): Organization of afferent input to subdivisions of area 8 in rhesus monkeys. J Comp Neurol 200:407–431.

Cavada C, Goldman-Rakic PS (1989): Posterior parietal cortex in rhesus monkey: II. Evidence for segregated corticocortical networks linking sensory and limbic areas with the frontal lobe. J Comp Neurol 287:422–445.

Cohen JD, Forman SD, Braver TS, Casey BJ, Servan-Schrieber D, Noll DC (1994): Activation of prefrontal cortex in a nonspatial working-memory task with functional MRI. Hum Brain Mapping 1:293–304.

Colby CL, Duhamel J-R, Goldberg ME (1993): Ventral intraparietal area of the macaque: Anatomic location and visual response properties. J Neurophysiol 69:902–914.

Colby CL, Duhamel J-R, Goldberg ME (1995): Occulocentric spatial representation in parietal cortex. Cereb Cortex 5:470–481.

Courtney SM, Ungerleider LG, Keil K, Haxby JV (1996): Object and spatial visual working memory activate separate neural systems in human cortex. Cereb Cortex 6:39–49.

D'Esposito M, Detre J, Alsop D, Shin RK, Atlas S, Grossman M (1995): The neural basis of the central executive system of working memory. Nature 378:279–281.

Distler C, Boussaoud D, Desimone R, Ungerleider LG (1993): Cortical connections of inferior temporal area TEO in macaque monkeys. J Comp Neurol 334:125–150.

Duhamel JR, Colby CL, Goldberg ME (1992): The updating of the representation of visual space in parietal cortex by intended eye movements. Science 255:90–92.

Duvernoy H (1991): The Human Brain, New York: Springer-Verlag.

Friedman HR, Goldman-Rakic PS (1994): Coactivation of prefrontal cortex and inferior parietal cortex in working memory tasks revealed by 2DG functional mapping in the rhesus monkey. J Neurosci 14:2775–2788.

Funahashi S, Bruce CJ, Goldman-Rakic PS (1989): Mnemonic coding of visual space in the monkey's dorsolateral prefrontal cortex. J Neurophysiol 61:331–349.

Fuster JM (1973): Unit activity in the prefrontal cortex during delayed-response performance: Neuronal correlates of transient memory. J Neurophysiol 63:811–831.

Fuster JM (1989): The Prefrontal Cortex, New York: Raven Press.

Fuster JM (1995): Memory in the Cerebral Cortex, Cambridge, MA: MIT Press.

Fuster JM, Jervey JP (1982): Neuronal firing in the inferotemporal cortex of the monkey in a visual memory task. J Neurosci 2:361–375.

Goldberg TE, Berman KF, Randolph C, Gold JM, Weinberger DR (1996): Isolating the mnemonic component in spatial delayed response: A controlled PET ^{15}O-labeled water regional cerebral blood flow study in normal humans. Neuroimage 3:69–78.

Goldman-Rakic PS (1987): Circuitry of primate prefrontal cortex and regulation of behavior by representational memory. In: Plum F (ed): Handbook of Physiology, Volume 5, the Nervous System. Bethesda, MD: American Physiological Society, pp 373–417.

Goldman-Rakic PS, Chafee M (1994): Feedback processing in prefronto-parietal circuits during memory-guided saccades. Soc Neurosci Abstr 20:335.

Goldman-Rakic PS, Chafee M, Friedman HR (1993): Allocation of function in distributed circuits. In: Ono T, Squire L, Raichle ME, Perret DI, Fukuda M (eds): Brain Mechanisms of Perception and Memory: From Neuron to Behavior. New York: Oxford Press; pp 445–456.

Grossman M, Crino P, Stern NM, Hurting HI, Reivich M (1992): Attention and sentence comprehension in Parkinson's disease: The role of the anterior cingulate cortex. Cereb Cortex 2:513–525.

Heilman KM, Sypert GW (1977): Korsakoff's syndrome resulting from bilateral fornix lesions. Neurology 27:490–493.

Jonides J, Smith EE, Koeppe RA, Awh E, Minoshima S, Mintun MA (1993): Spatial working memory in humans as revealed by PET. Nature 363:623–625.

Kawamura K, Naito J (1984): Corticortical projections to the prefrontal cortex in the rhesus monkey investigated with horseradish peroxidase techniques. Neurosci Res 1:89–103.

Lueschow A, Miller EK, Desimone R (1994): Inferior temporal mechanisms for invariant object recognition. Cereb Cortex 4:523–531.

McCarthy G (1995): Functional neuroimaging of memory. Neuroscientist 1:155–163.

McCarthy G, Blamire AM, Puce A, Nobre AC, Bloch G, Hyder F, Goldman-Rakic P, Shulman RG (1994): Functional magnetic resonance imaging of human prefrontal cortex activation during a spatial working memory task. Proc Natl Acad Sci USA 91:8690–8694.

McCarthy G, Adrignolo A, Spicer M, Luby M, Gore J, Allison T (1995): Localized brain activation associated with visual stimulus motion studied by functional magnetic resonance imaging in humans. Hum Brain Mapping 2:134–243.

McCarthy G, Puce A, Constable RT, Krystal JH, Gore JC, Goldman-Rakic P (1996): Activation of human prefrontal cortex during spatial and object working memory tasks measured by functional MRI. Cereb Cortex 6:600–611.

Miller EK, Desimone R (1994): Parallel neuronal mechanisms for short-term memory. Science 263:520–522.

Owen AM, Evans AC, Petrides M (1996): Evidence for a two-stage model of spatial working memory processing within the lateral frontal cortex: A positron emission tomography study. Cereb Cortex 6:31–38.

Pardo JV, Pardo PJ, Janer KW, Raichle ME (1990): The anterior cingulate cortex mediates processing selection in the Stroop attentional conflict paradigm. Proc Natl Acad Sci USA 87:256–259.

Petrides M, Alivisatos B, Evans AC, Meyer E (1993a): Dissociation of human mid-dorsolateral from posterior dorsolateral frontal cortex in memory processing. Proc Natl Acad Sci USA 90:873–877.

Petrides M, Alivisatos B, Meyer E, Evans AC (1993b): Functional activation of human frontal cortex during the performance of verbal working memory tasks. Proc Natl Acad Sci USA 90:878–882.

Posner MI, Inhoff AW, Friedrich FJ, Cohen A (1987): Isolating attentional systems: A cognitive-anatomical analysis. Psychobiology 15:107–121.

Puce A, Allison T, Gore JC, McCarthy G (1995): Face-sensitive regions in human extrastriate cortex studied by functional MRI. J Neurophysiol 74:1192–1199.

Puce A, Allison T, Asgari M, Gore JC, McCarthy G (1996): Differential sensitivity of human visual cortex to faces, letterstrings, and textures. J Neurosci 16:5205–5215.

Quintana J, Yajeya J, Fuster JM (1988): Prefrontal representation of stimulus attributes during delay tasks. I. Unit activity in cross-temporal integration of sensory and sensory-motor information. Brain Res 474:211–221.

Rao SC, Rainer G, Miller EK (1997): Integration of what and where in the primate prefrontal cortex. Science 276:821–824.

Selemon LD, Goldman-Rakic PS (1988): Common cortical and subcortical targets of the dorsolateral prefrontal and posterior parietal cortices in the rhesus monkey: Evidence for a distributed neural network subserving spatially guided behavior. J Neurosci 8:4049–4068.

Smith EE, Jonides J, Koeppe RA, Awh E, Schumacher E, Minoshima S (1995): Spatial vs. object working memory: PET investigations. J Cogn Neurosci 7:337–358.

Smith EE, Jonides J, Koeppe RA (1996): Dissociating verbal and spatial working memory using PET. Cereb Cortex 6:11–20.

Sutherland RJ, Hoesing JM (1993): Posterior cingulate cortex and spatial memory: A microlimnology analysis. In: Vogt BA, Gabriel M (Eds): Neurobiology of the Cingulate Cortex and Limbic Thalamus: A Comprehensive Handbook. Boston: Birkhauser, pp 461–477.

Swartz BE, Halgren E, Fuster J, Mandelkern M (1994): An FDG-PET study of cortical activation during a short-term visual memory task in humans. Neuroreport 5:925–928.

Swartz BE, Halgren E, Fuster J, Simpkins F, Gee M, Mandelkern M (1995): Cortical metabolic activation in humans during a visual memory task. Cereb Cortex 3:205–214.

Talairach J, Tournoux P (1988): Co-Planar Stereotaxic Atlas of the Human Brain, New York: Thieme.

Ungerleider LG, Mishkin M (1982): Two cortical visual systems. In: Ingle DJ, Goodale RJ, Mansfield W (eds): Analysis of Visual Behavior. Cambridge, MA: MIT Press, pp 549–586.

Valenstien E, Bowers D, Verfaillie M, Heilman KM, Day A, Watson RT (1987): Retrosplenial amnesia. Brain 110:1631–1646.

Webster MJ, Bachevalier J, Ungerleider LG (1994): Connections of inferior temporal areas TEO and TE with parietal and frontal cortex in macaque monkeys. Cereb Cortex 5:470–483.

Wilson FA, O'Scalaidhe SP, Golman-Rakic PS (1993): Dissociation of object and spatial processing domains in primate prefrontal cortex. Science 260:1955–1958.

Zatorre RJ, Evans AC, Meyer E, Gjedde A (1992): Lateralization of phonetic and pitch processing in speech perception. Science 256:846–849.